RAYMOND M. SOVA, BARRY E. GRABOW, and BRADLEY G. BOONE

HIGH-TEMPERATURE SUPERCONDUCTING ELECTROMAGNETIC RADIATION DETECTORS

Detection of electromagnetic energy is one of the most promising near-term applications for high-temperature superconducting materials. Research and development in the Electro-Optical Systems Group at the Applied Physics Laboratory have focused on creating thin-film detectors using such materials. This article summarizes our work in the development of two types of detectors: a bolometric infrared detector and a nonbolometric microwave detector. The possible physical mechanisms for microwave detection are also discussed.

INTRODUCTION

The development of high-temperature superconducting (HTSC) thin-film devices for electro-optical and radio-frequency sensors is probably one of the most likely near-term outcomes of recent breakthroughs in the field of superconductivity.[1] Among the many potential devices being considered, passive thin-film devices, which can be used as detectors of electromagnetic radiation, are favored. High-temperature superconducting materials are expected to exhibit excellent performance as quantum (Josephson junction) radiation detectors at extremely high frequencies reaching into the far-infrared band; the performance of these detectors will be limited ultimately by the very high superconducting energy gap found in HTSC materials (≤50 meV) (see the boxed insert entitled "A Quick Tutorial on Superconductivity"). High sensitivity is also expected for these types of detectors ($\leq 10^{15}$ photons/cm^2·s in a 1-kHz bandwidth for a 10^{-4} cm^2 detector area as calculated by Forrester and Talvacchio[2]). Fabrication of prescribed (ideal) Josephson junctions is, however, very difficult because the junction size must be on the order of the coherence length, which is extremely short and anisotropic in these materials.

Alternatively, bolometers based on HTSC materials have been proposed[3] because they are relatively easy to fabricate. They operate on the principle that incident radiation of virtually any wavelength will induce a resistive transition from a superconducting state to a normal state in a thin piece of superconducting film. The substrate must be coupled to a thermal reservoir and have a low heat capacity to yield the best possible response to incident radiation in the shortest possible time. Thus, a trade-off between response time and sensitivity in bolometric detectors exists that limits their performance relative to ideal quantum detectors. Better performance should be obtained, however, by making the HTSC bolometric element very small and impedance-matching it to an efficient antenna structure. Calculated ideal sensitivity[3] (measured by noise equivalent power [NEP]) is in the range of 1 to 20 × 10^{-12} W/Hz$^{1/2}$ (see the boxed insert entitled "Important Detector Performance Parameters").

Granular film (multiple Josephson junction) detectors, on the other hand, may be competitive as electromagnetic detectors, as suggested by Wolf.[4] Granular films also appear to display nonbolometric behavior stemming, probably, from multiple weak links. Several investigators have also studied the possible nonbolometric response mechanisms of HTSC thin films. Konopka et al.[5,6] and Jung et al.[7] have measured the microwave response of yttrium–barium–copper oxide (YBCO) and bismuth–strontium–calcium–copper oxide (BSCCO) films and clearly observed nonbolometric behavior in YBCO films. A nonbolometric mechanism may be a better means of making a detector—particularly for microwave frequencies.

Research at APL has covered a wide range of fundamental issues and device applications since the discovery of the HTSC materials.[8,9] This article focuses on our work in the development of HTSC electromagnetic detectors. Originally, we began with the development of a superconducting bolometer, since it was clearly the most straightforward application for HTSC materials. During our testing of various films, a large nonbolometric response was observed when the samples were illuminated with microwaves. Since then, more thorough measurements have been made that indicate the nonbolometric response can support a very fast wideband detector. Thus, the emphasis of our current research has shifted to understanding the nonbolometric response mechanism, although we are still interested in development of the bolometric detector. Various issues involved with the design, development, and testing of both the bolometric and nonbolometric detectors are discussed in this article. The performance of both detectors is compared with that of standard detectors. The results indicate that an HTSC bolometer is competitive with a pyroelectric detector in the infrared spectral region, and an HTSC nonbolometric

A QUICK TUTORIAL ON SUPERCONDUCTIVITY

The two most fundamental properties of superconductors are zero dc resistance and the Meissner effect, both of which occur at temperatures below a critical temperature T_c. The Meissner effect is the ability of cooled superconductors to expel static magnetic fields (i.e., perfect diamagnetism) up to a critical field H_c. Actually, the superconducting state of a material is associated with the values of three parameters: temperature, current, and magnetic field. The superconducting state can be destroyed by exceeding the critical value of any one of these parameters.

In a normal metal, electrons are essentially unbound and free to move through the crystal lattice. Electron collisions with the lattice are the source of resistance and the basis of temperature-dependent losses in metals. In superconductors, when the crystal lattice is cooled to near the critical temperature T_c, electrons of opposite momentum and spin near the Fermi energy condense into bound pairs (with a lower, more favorable energy) called Cooper pairs, which exhibit zero dc resistance. The superconducting energy gap Δ is the the binding energy of the paired electrons and is also the gap that separates the sea of quasiparticles (normal electrons) from the bound pairs in the conduction band.

The superconducting state is also characterized as a collective quantum phenomenon in which the wave function

$$\Psi = |\Psi| \exp(j\phi) \qquad (1)$$

is a complex quantity that describes the macroscopic superconducting state. The modulus $|\Psi|$ is the superconducting order parameter and ϕ is the phase. The modulus squared $|\Psi|^2$ is n_p, the number density of Cooper pairs that constitute the supercurrent. The superconducting energy gap Δ is proportional to n_p and is typically 50 meV or less for high-temperature superconducting (HTSC) materials.

Two key length-scale parameters used to describe the superconducting state are the coherence length and London penetration depth. The coherence length ξ_0 is a measure of the distance over which the superconducting order parameter varies, where $\xi_0 \propto 1/\Delta$. The coherence length can also be viewed as the size of a Cooper pair. For HTSC materials, coherence length is very small (typically ≤ 2.7 nm). The London penetration depth λ_L is defined as the distance a magnetic field will penetrate into the superconductor, where $\lambda_L \propto 1/n_p^{1/2}$. For HTSC materials, the London penetration depth is approximately 200 nm.

A superconducting ring will trap flux within it when a magnetic field is present and the structure is cooled below T_c. This phenomenon is an important fundamental property for device applications. The trapped flux will induce (because of the Meissner effect) a persistent circulating (shielding) current through a depth equal to λ_L surrounding an area of superconducting material with a diameter at least on the order of the coherence length. The phase of the superconducting wave function changes by $2\pi n$ in going once around the ring, resulting in the quantization of the magnetic flux as measured in units of flux quanta, $\Phi_0 = h/2e = 2 \times 10^{-15}$ Wb, where h is Planck's constant and e is the electron charge. These flux quanta manifest themselves as vortices or fluxons, especially in certain types of thin films.

Another fundamental effect noted in superconductors of practical importance for devices is the Josephson effect, which is observed when two pieces of superconductor are separated by a thin region of weak metallic superconductor (where the order parameter is reduced) or by an insulator through which Cooper pairs can tunnel. The Josephson critical current I_c is the largest flow of Cooper pairs allowed through the junction without losses. When a current less than I_c flows through the junction, Cooper pairs tunnel through the barrier, establishing a phase change ($\Delta\phi$) between the wave functions on each side of the junction, which results in a current given by

$$I = I_c \sin \Delta\phi \, . \qquad (2)$$

When I exceeds I_c, the phase difference evolves in time according to

$$d\Delta\phi/dt = 4\pi eV/h \, , \qquad (3)$$

where V is the voltage across the junction and h is Planck's constant, and then current no longer flows without losses. In this situation, an ac component of current is added to I_c at a frequency proportional to the voltage across the junction. Josephson junctions exhibit inherent nonlinear properties that can be used in the detection of radiant energy.

detector may be competitive with a Schottky diode in the microwave spectral region. Applications for both detectors are also discussed.

DETECTOR THEORY

Superconducting detectors of radiant energy use the dependence of resistance on temperature or current as a detection mechanism.[10] This change of resistance is measured as a change in sample voltage. What follows is a simplified explanation of this response process. In general, a voltage change dV can occur in a piece of superconductor as the result of a change in temperature T (indirect thermal response) and/or a change in the junction critical current I_c via the superconducting energy gap Δ (direct electron interaction response) caused by incident electromagnetic radiation of power P. This change is given by

$$dV = \underbrace{I_B(\partial R/\partial T)(\partial T/\partial P)dP}_{\text{Bolometric Term}} + \underbrace{(\partial V/\partial I_c)(\partial I_c/\partial \Delta)(\partial \Delta/\partial P)dP}_{\text{Nonbolometric Term}} + \underbrace{V_n}_{\text{Noise Term}} , \qquad (1)$$

where the third term V_n is the noise voltage due to fluctuations in the bias current I_B, bath temperature T, and incident power P. The first term of Equation 1 represents the bolometric response, and the second term denotes the nonbolometric response.

IMPORTANT DETECTOR PERFORMANCE PARAMETERS

A block diagram of a generic high-temperature superconducting (HTSC) detector is shown in the figure. Incident photon flux P_s illuminates a detector of area A and creates an output signal voltage V_s by one or more detection mechanisms (see Detector Theory section). Various noise sources add statistically to produce a cumulative output noise voltage V_n. These noise sources include photon, detector, and preamplifier noise. The following detector parameters are used to quantify a detector's performance in terms of these measured quantities:

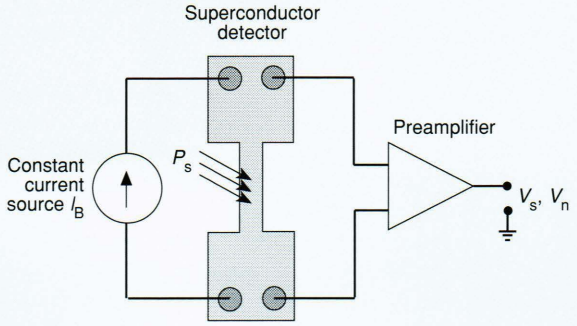

Block diagram of a generic high-temperature superconducting (HTSC) detector. The output signal voltage V_s is produced by incident radiation power P_s. Output noise voltage V_n is produced by noise from incident radiation, the detector, and the preamplifier. The detector bias current is designated I_B.

1. Responsivity, $\Re = V_s/P_s$ (in V/W), is the ratio of the ouput signal voltage to incident photon flux. A good value is 1000 V/W.

2. The detector bandwidth defines the output electrical bandwidth Δf(in Hz) of the detector system. Usually, the detector bandwidth is minimized to reduce output noise V_n. The value of the bandwidth depends on the application.

3. The noise equivalent power, NEP = $V_n/\Re$ (in W/Hz$^{1/2}$), is the amount of incident photon flux required to produce a signal-to-noise ratio of 1 at the output of a detector in a 1-Hz detector bandwidth. A lower NEP implies better performance. A good value is $\leq 10^{-10}$ W/Hz$^{1/2}$.

4. The dynamic range, $DR_{dB} = 10 \log(P_{max}/P_{min})$, is the range of input powers P_{min} to P_{max} in which the output voltage V_s is linearly related to the input power P_s. Usually the dynamic range is expressed in decibels. Typical values range from 30 to 40 dB.

5. The detector time constant τ (in s) defines how quickly the detector can respond to changes in the incident photon flux level. A fast detector has a small time constant (usually in the nanosecond range).

6. The spectral range $\Delta\lambda$ is the electromagnetic spectral band in which the detector can operate (usually, the wider the spectral range, the better).

The first two components of the bolometric term are the current bias I_B and the derivative of the resistance curve (dR/dT). The third component of the bolometric term ($\partial T/\partial P$) is equal to $1/G$, where G is the thermal conductance.

Bolometric detection is caused by a change in a sample's resistivity when the sample is heated by incident radiation. A superconducting material cooled to the critical temperature T_c will change from the normal state to the superconducting state in a very small temperature interval ΔT. The very large value of dR/dT that occurs in the transition region is used for bolometric detection.[11] Such a device is called a "transition edge" bolometer. It is operated by holding its temperature at the center of the transition region under background radiation. When an incident signal is present, the bolometer is heated to a higher temperature, which causes an increase in resistance. The resistance change is converted to an output voltage change by biasing the device with a constant current source. The output response voltage is directly proportional to dR/dT, as shown in Equation 1.

When considering the nonbolometric term, a major simplifying assumption is that the critical current I_c and the energy gap Δ are independent of temperature changes caused by the incident radiation. This assumption amounts to separating I_c and Δ into temperature- and power-dependent terms. The first two components of the nonbolometric term ($\partial V/\partial I_c$) and ($\partial I_c/\partial \Delta$) can be evaluated on the basis of the type of junction being modeled in the film. The third component ($\partial \Delta/\partial P$) depends on the mechanism behind the direct change in the superconducting energy gap due to incident radiant energy, which is the subject of our current analytical investigations.

Nonbolometric detection of radiant energy in superconductors can occur as the result of several possible mechanisms: directly via the Josephson effect, by breaking Cooper pairs under nonequilibrium conditions, and by classical rectification (video or square-law detection).[12] Many recent investigations[5-7,13-16] ascribe the measured results with the HTSC films to a random network of Josephson junctions in which each junction is modeled as having two currents: a supercurrent (Cooper pairs) and a normal current (quasiparticles). It is also possible that incident radiation may couple to existing vortices created by the bias current and thereby induce increased dissipation.[17-22]

Another way to view the detection process in small junctions is to visualize a long strip of superconductor having a width less than the coherence length (one-dimensional film too narrow to contain a fluxon). Superconductivity will break down in this film where the magnitude of the energy gap is locally reduced by incident photons, causing "phase-slip" centers where the phase of the wave function repeatedly slips through 2π. The phase slip then induces a voltage in the junction (first boxed insert, Eq. 3) and can cause the entire strip to switch thermally much like a transition edge bolometer. If the strip is short and there is no thermal bottleneck,

however, then the Josephson effect should manifest itself in a virtually sinusoidal current-phase relation (first boxed insert, Eq. 2).

The property of perfect diamagnetism can be compromised in HTSC devices by the creation of vortices that represent the mode of partial penetration of a magnetic field into a continuous superconductor such as a thin film. Lattice defects in the sample can pin these vortices in a close-packed array. Sufficiently large transport currents in the sample can depin the vortices through Lorentz forces. In wider junctions (wider than the coherence length or the penetration depth, depending on the type of film), multiple fluxons can exist. When a piece of film is current biased, the vortices flow through the junction transversely to the dc transport current, causing dissipation and resistive losses. The dissipation is generally described as "flux creep" when the pinning forces dominate and "flux flow" (vortex flow) when Lorentz forces dominate. Additional flux-flow resistance caused by incident radiant energy driving areas of a junction normal can be used as a detection mechanism.

Granular thin films, or films that are thinner than the London penetration depth (referred to as two-dimensional films), can exhibit a vortex–antivortex creation phenomenon even in the absence of applied magnetic fields (or their sources within the film: applied dc currents).[18] In this process, the film goes through a phase transition near T_c, where the film resistance approaches zero. This effect is called the Kosterlitz-Thouless (KT) transition, where vortex (clockwise-circling shielding currents) and antivortex (counterclockwise-circling shielding currents) pair excitations are bound for $T < T_c$. These bound vortex–antivortex pairs have zero resistance at low temperatures (below the KT transition temperature T_{KT}) even if they are not pinned. The dissociation of the bound pairs can be assisted by radiant energy impinging on the film. Vortex–antivortex pairs that are broken are dissipative and cause resistive losses. This vortex–antivortex pair dissociation process can be a means of detection.[13,20-22]

DETECTOR DESIGN AND OPTIMIZATION

Our research has focused on using the bolometric and nonbolometric detection mechanisms for infrared and microwave detectors, respectively. The issues involved in designing and optimizing each detector are discussed in this section. The bolometric detector requires that a thin superconducting film with a very narrow transition width ΔT be deposited on a substrate with a very small heat capacitance. The nonbolometric detector requires a granular superconducting film with a wide transition width and a resistive tail. Details of the design methodology for each detector are given below.

Bolometric Detector Design

Because of the trade-off between the detector time constant τ and sensitivity NEP, a bolometer must be designed for a specific application. The application for our HTSC bolometer is a Fourier transform spectrometer (FTS). Our goal is to build a bolometer that operates in the far-infrared spectral band and is at least as sensitive as a pyroelectric detector. Requirements for this bolometer are as follows: NEP $< 5\times10^{-9}$ W/Hz$^{1/2}$, $\tau = 10$ ms, spectral range $\Delta\lambda = 10$ to 1000 μm, and area = 4 mm^2. This design will be thermally isolated to achieve the desired response time and interfaced to a low-temperature junction-field-effect-transistor (JFET) preamplifier (preamp) to achieve low noise.

The classical bolometric model[23] was implemented on a computer and used to calculate the bolometer parameters required to achieve the desired values of τ and NEP. In a properly optimized bolometer, the time constant is given by

$$\tau = C/G \ , \tag{2}$$

where C is the heat capacitance of the bolometer, and G is the thermal conductance path between the bolometer and the cold head.

Photon, detector, and preamp noises contribute to the NEP of a bolometer. The photon and preamp noise terms are reduced by using a 77-K spectral filter and a 77-K low-noise preamp, respectively. The preamp noise is further reduced by optimizing the film resistance R. The detector noises include phonon (temperature fluctuations), Johnson (electrical fluctuations), and $1/f$ (material-dependent noise). The $1/f$ noise is negligible for high-quality HTSC films[24] and can be eliminated by operating at finite modulation (chopper) frequencies.

The NEP of an optimized bolometer is essentially equal to the root-sum-square of the NEP's due to phonon and Johnson noise. To minimize the NEP, the Johnson noise term is equated to the phonon noise term by adjusting the chopping frequency. The resulting NEP, expressed in terms of the phonon noise, is given by

$$\text{NEP} = (8kT_b^2G)^{1/2} \ , \tag{3}$$

where k is Boltzmann's constant and T_b is the bolometer temperature.

Equations 2 and 3 state the fundamental trade-off between τ and NEP, which is solely dependent on the thermal properties (C and G) of the bolometer. Minimization of the heat capacitance C is one of the major issues in the design of a sensitive HTSC bolometer. The substrate of the bolometer usually limits the value of C. Ideally, one would like to use a very small substrate made out of a material with a small specific heat.[3] Once C is minimized, the value of G can be adjusted using Equations 2 and 3 to provide the proper values of τ and NEP. Although there is a lower limit on G caused by bolometric heating due to background radiation,[3] this limit is not reached in our design.

Ideally, we would like the radiation absorption of the bolometer to be as large and as flat as possible over the entire spectral range of operation (10 to 1000 μm). It has been shown that a thin metal film deposited onto a substrate can absorb 50 to 60% of the incident radiation over the spectral range from dc to visible with a relatively flat response.[25] The thickness of the film is chosen such that the sheet resistance $R_\square$ is equal to 60π. (The sheet resistance may be calculated as $R_\square = 1/\sigma d$, where σ is the electrical conductivity of the film and d is the film thickness. The sheet resistance is a measure of the film resistance encountered by incident radiation.) For our bolom-

eter, the radiation absorber will consist of a bismuth film deposited onto one side of the detector substrate.

Figure 1 presents a diagram of our proposed bolometer design, which consists of a very small substrate with an HTSC thin-film thermometer deposited on one side and a bismuth thin-film radiation absorber deposited on the opposite side. The bolometer is suspended from an alumina carrier by four gold wires, which are attached to the HTSC film by silver paste. The length and diameter of the wires are chosen to provide an optimal thermal conductance path from the bolometer to the cold head (to optimize G). They also serve as electrical connections to the bolometer.

The smallest $SrTiO_3$ substrates that we have been able to obtain for our bolometer are $2 \times 2 \times 0.125$ mm in size. Epitaxial YBCO films (300 nm thick) were deposited onto these substrates. Preliminary resistance measurements indicate these films have very good superconducting properties and are suitable for bolometric detectors. Using the bolometric model, the following theoretical detector characteristics were calculated for these films: NEP $\sim 10^{-10}$ W/Hz$^{1/2}$ and $\tau \sim 10$ ms. By thinning the substrates even more, the NEP can be improved by a few orders of magnitude,[26] although this is a challenging task.

Microwave Detector Design

Our initial application for the nonbolometric detector, which was chosen to demonstrate the potential of its detection mechanism, is a microwave power detector operating in X band (8 to 12 GHz). Future applications may entail using the device in the millimeter, submillimeter, or far-infrared regions. Figure 2 is a diagram of our antenna/detector assembly. A spiral antenna (Fig. 2A) designed to operate over the 2- to 12-GHz band will be used to couple the incident radiation to the small detector (2×2 mm) optimally. The detector is mounted in the center of the spiral antenna and biased with two leads that pass through holes to a current source (Fig. 2B). The detector voltage leads are connected directly to the antenna.

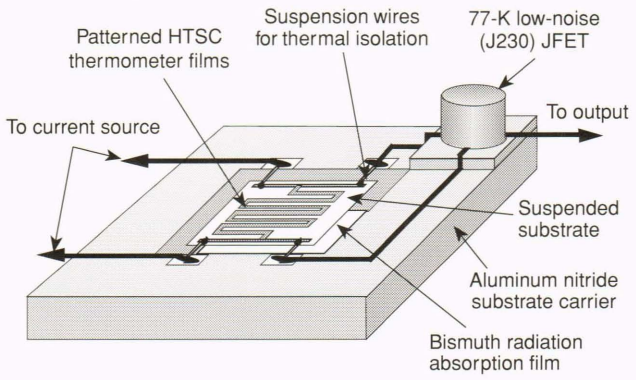

Figure 1. Conceptual prototype high-temperature superconducting (HTSC) bolometer consisting of a very thin substrate suspended by very small wires for thermal isolation. A bismuth absorption film and a patterned HTSC thermometer film are deposited on opposite sides of the substrate. A 77-K junction field effect transistor (JFET) is connected to the detector output to minimize detector noise.

Our preliminary experimental results on simple HTSC films have shown that the microwave response improves with increasing transition width ΔT and sheet resistance $R_\square$ (see the Measurement Results section). Optimization of the HTSC film will therefore involve producing granular films with wide transition widths and large sheet resistances. The detector resistance should again be $60\pi\ \Omega$ to optimize coupling between the antenna and the detector.[27] Further requirements for the nonbolometric detector will emerge when the detection mechanism is better understood.

FABRICATION AND INTERFACING

Details of the thin-film fabrication steps used in developing both the bolometric and nonbolometric detectors are given in this section These steps include film depositing and annealing, creating low-resistance ohmic contacts, and patterning.

The growth of an HTSC thin film is very complex and is governed by many parameters, including film stoichiometry, substrate type, and deposition and annealing methods. Over the past several years, researchers have optimized these parameters and produced high-quality HTSC thin films by a variety of deposition techniques such as laser ablation, magnetron sputtering, coevaporation, and molecular beam epitaxy.[28,29] Two methods of film growth are postdeposition annealing and *in situ* (i.e., during deposition) growth.

For postdeposition annealing, a film is deposited onto a substrate held at a low temperature (typically <300°C). The deposited film is amorphous, and a high postdeposition annealing temperature (typically >850°C) is required to grow the superconducting crystal structure. The high-temperature processing causes the nucleation and growth of stoichiometric grains surrounded by nonstoichiometric grain boundaries. The grain sizes are generally tens of micrometers, and the grain boundaries are hundreds of nanometers (i.e., much larger than the coherence length).[30] The granular films produced by postdeposition annealing usually have low critical currents, low transition temperatures, and wide transitions (ΔT).

For *in situ* growth, a film is deposited onto a heated substrate (typically >600°C) in a high-oxygen atmosphere. The high substrate temperature activates epitaxial growth during deposition. (Epitaxial growth occurs when the crystal lattice of the film aligns itself to the crystal lattice of the substrate. For proper growth, the lattice dimensions of the substrate need to be compatible with those of the film. Substrates compatible with the HTSC material include $LaAlO_3$, $SrTiO_3$, and $LaGaO_3$.) The deposited film is superconducting and does not require postdeposition annealing. Epitaxial films produced by *in situ* growth are very smooth and have very good superconducting properties (i.e., large critical currents, high transition temperatures, and very sharp transitions).

For our research, we obtained HTSC thin films from both university research laboratories (including APL) and commercial vendors. We studied both granular and epitaxial YBCO films along with granular BSCCO films. Film thicknesses were typically around 1 μm. The films were deposited on a variety of substrates, including magnesium

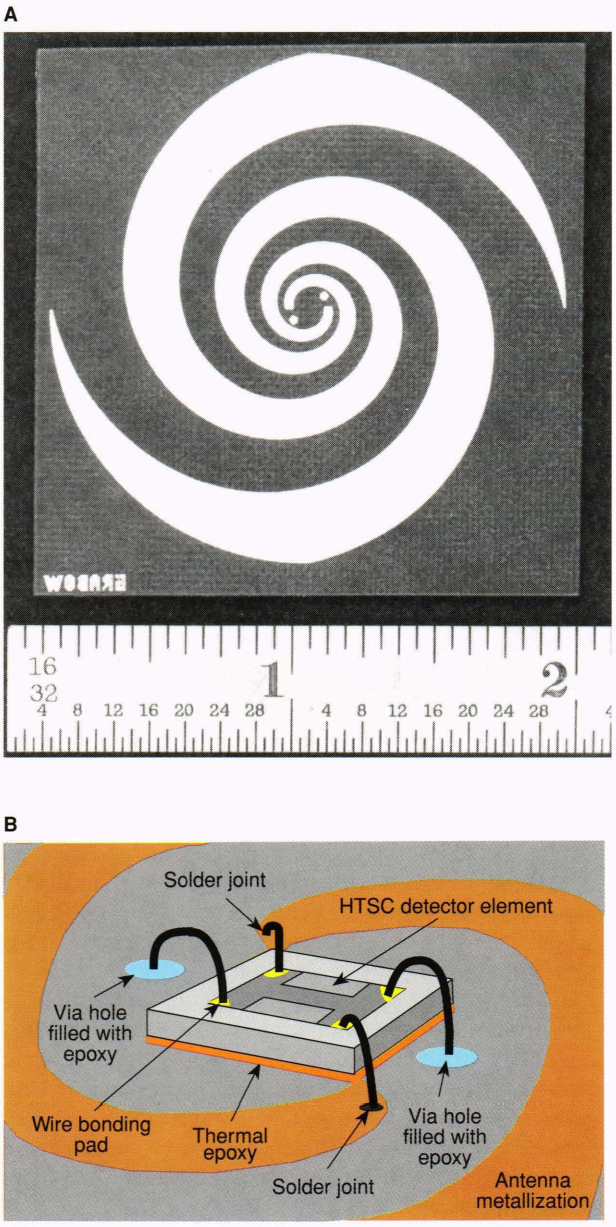

Figure 2. Antenna/detector assembly. **A**. Plan view of a 2- to 12-GHz spiral antenna. **B**. Close-up view of coupling to a high-temperature superconducting (HTSC) detector element.

oxide (MgO), cubic zirconia (ZrO_2), strontium titanate ($SrTiO_3$), and lanthanum aluminate ($LaAlO_3$).

The epitaxial film (about 300 nm thick) was produced by depositing YBCO on an $SrTiO_3$ substrate at 735°C using magnetron sputtering. The deposition was performed in oxygen for *in situ* growth. Figure 3A is a photograph of the resulting film, and Figure 3B is the resistance versus temperature curve for this film. The film is very smooth with no signs of granularity. The room temperature resistivity is about 3 $\mu\Omega$·cm. The resistance has a metallic behavior above T_c (i.e., resistance decreases linearly with decreasing temperature) and a very narrow transition width ($\Delta T \sim 1$ K) at T_c. No signs of a resistive tail at temperatures below T_c are evident.

The granular film was produced by depositing BSCCO onto an MgO substrate at 300°C using laser ablation[31] and postdeposition annealing. The annealing schedule consisted of a 25 to 880°C ramp up for 1 h, a soak at 880°C for 10 min, and an 880 to 25°C ramp down for 3 h. The film thickness is about 2 μm, and average grain size is estimated at 50 μm. Figure 4A is a photograph of the film, and Figure 4B is the resistance versus temperature curve for this film. The film has a nonuniform granular morphology. The room temperature resistivity is greater than 9200 $\mu\Omega$·cm. The resistance has a weak metallic behavior for temperatures above T_c, as indicated by the fairly constant resistance versus temperature curve in this region. The transition region is very broad (transition width of about 10 K), and a large resistive tail is found in the region below the transition.

The epitaxial film is well suited for the bolometric detector, since it has a very narrow transition width. The granular film is well suited for the nonbolometric detector because of its broad transition width, large resistive tail, and high resistivity. We have done annealing experiments with granular films and have shown that the transition widths and resistive tail spreads can be made larger by annealing at high temperatures.

Ohmic contacts with very low resistance are essential in the development of a highly sensitive detector, since noise from high-resistance contacts will ruin the sensitivity of the detector. Two methods for depositing contacts have been successful. The first method entails applying small silver epoxy contacts to a film and annealing it at a high temperature. The annealing schedule consists of a 25 to 500°C ramp up for 1 h, a 500 to 820°C ramp up for 5 h, and an 820 to 25°C ramp down for 1 h. During annealing, the organic binder of the epoxy evaporates, and the silver diffuses into the film, producing a strong mechanical bond and a good ohmic contact. These contacts are very robust. For example, one sample was temperature cycled between 300 and 13 K more than twenty times, and the contact resistance remained constant. Typical contact resistances varied from a few ohms at 300 K to approximately 0.1 Ω at 13 K. This method of depositing contacts is currently being used for preliminary devices.

The second method for producing ohmic contacts involves evaporating gold through a shadow mask. First, plasma etching is used to remove a thin oxide layer that forms on the film when exposed to air. Then 400 nm of gold is immediately deposited onto the film. Although this method has produced good ohmic contacts, the gold contacts do not strongly adhere to the films. (The gold contacts were pulled completely off the film during several attempts at wire bonding.) Future work will focus on evaporating silver and annealing the silver contacts at high temperatures to produce a strong mechanical bond.

Several patterning techniques have been tried, including *in situ* deposition masking, wet-chemical etching, and laser patterning. These methods are available individually or in combination to pattern complex planar structures such as meanderlines and microstrip. *In situ* masking was our earliest attempt at patterning, and it was used to achieve 625-μm line widths, which are sufficient to make

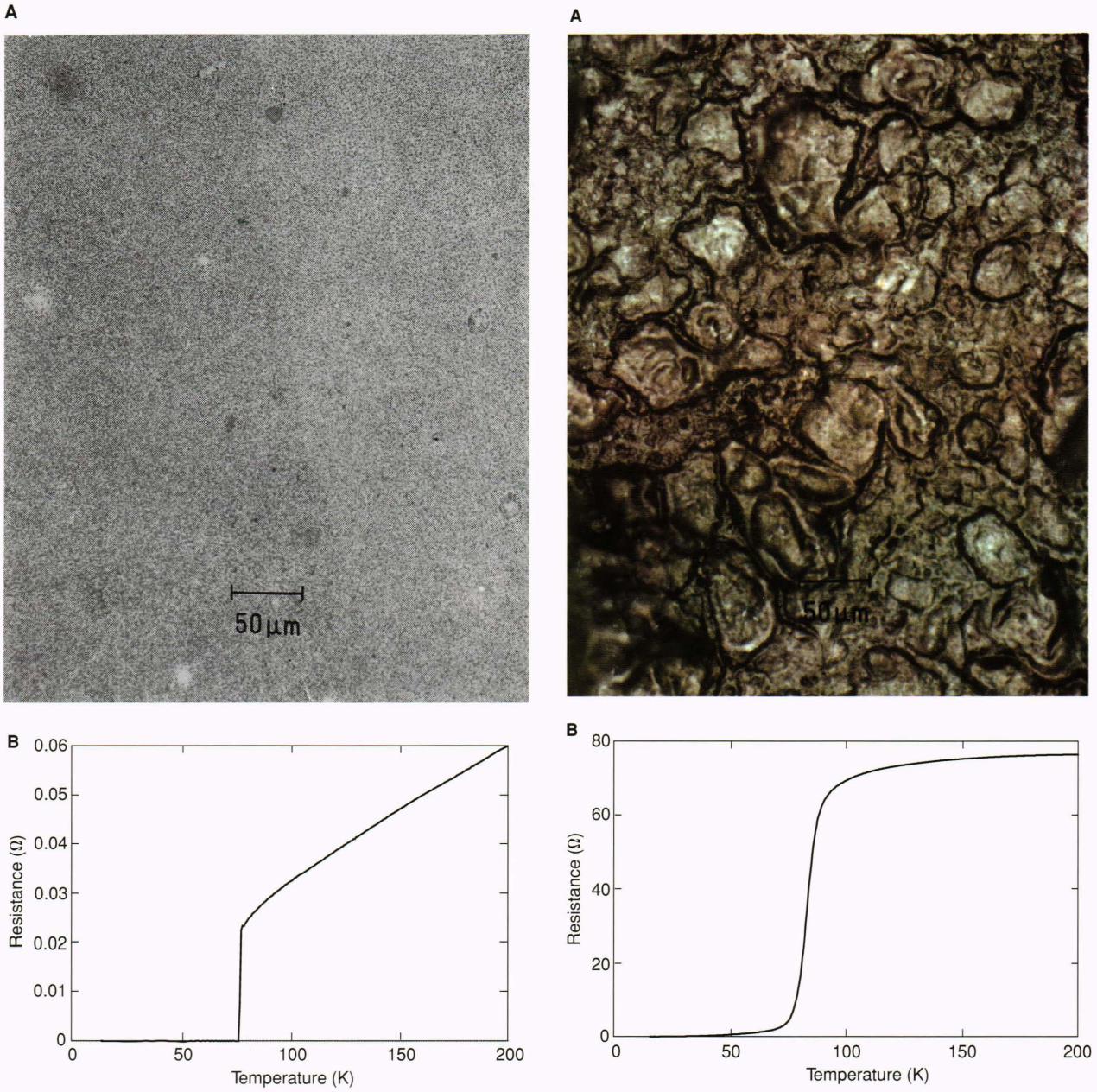

Figure 3. Characteristics of a high-quality epitaxial high-temperature superconducting thin film. **A**. Optical microscope photograph of a very smooth epitaxial yttrium–barium–copper oxide thin film (SCC3B). The average grain size is ~50 μm. **B**. The corresponding resistance versus temperature curve. The transition width is very narrow (<1K), and no resistive tail is observed below the transition region. (Resistivity at 300 K = 3.0 $\mu\Omega$•cm, transition temperature ~90 K, bias current = 500 μA.)

Figure 4. Characteristics of a granular high-temperature superconducting thin film. **A**. Optical microscope photograph of a granular bismuth–strontium–calcium–copper oxide thin film (LAP10F). The average grain size is ~50 μm. **B**. The corresponding resistance versus temperature curve. The transition width is very broad (~10 K), and a large resistive tail is present. (Resistivity at 300 K = 9200 $\mu\Omega$•cm, transition temperature ~83 K, bias current = 89.8 μA.)

simple detector elements and striplines. A 50-μm-thick Kovar mask was used. The limitations of using a shadow mask are that line widths are limited to 50 μm or more, and complex patterns cannot be made. Thus, procedures for wet-chemical etching of BSCCO films were developed. These procedures involve using a Shipley 21822 photoresist and choosing an acid etch. Choice of the acid etch depends on film type (YBCO or BSCCO) and whether the film has previously been annealed. Line widths of 1 μm can be achieved.

To achieve finely controlled, complex patterns on very small substrates (~1 × 1 mm), a laser patterning system was developed as shown in Figure 5.[26] Similar efforts by other groups have been applied to YBCO films.[32,33] Rothschild et al.[32] and Liberts et al.[33] have shown that the film can be locally heated and consequently annealed by ex-

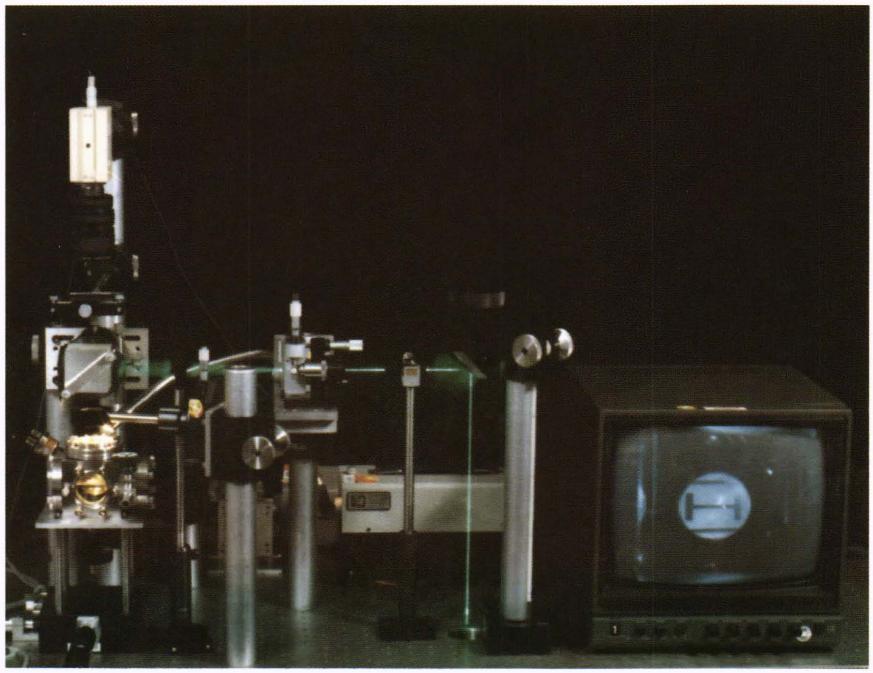

Figure 5. Argon laser patterning system developed for sketching and locally annealing patterns on high-temperature superconducting thin films.

posing the film to a laser beam in an oxygen atmosphere. By using a reducing atmosphere (including nitrogen), an initially superconducting film can be driven back into the normal phase. For our preliminary testing, we increased the laser power to a relatively low threshold level so that the film could actually be etched in ambient air. Thus, finely sketched (computer-controlled) patterns can be produced on substrates too small to be patterned by conventional wet-chemical etch procedures. This approach employs an argon ion laser operated at 514.5 nm with a $\leq$10-μm spot size and 7×10^5 W/cm^2 maximum irradiance on the substrate. Laser modulation occurs electromechanically. Substrate positioning is achieved with a computer-controlled x-y translation stage that has a 0.1-μm stepping resolution. A vacuum cell with multiaxis optical access is used to house the film. Partial pressure of oxygen and/or nitrogen from about 100 mTorr to one atmosphere can also be maintained during operation to explore local annealing of BSCCO films. The sample is monitored under reflected ambient light using a charge-coupled-device camera and telephoto/zoom lens combination, and the transmitted power is measured with a photodetector.

To demonstrate the use of the laser patterning system, meanderline patterns were sketched onto a variety of YBCO and BSCCO thin films. As an example, Figure 6 shows a meanderline pattern that was etched onto a 1-μm-thick granular YBCO film. The laser was guided by computer between the two closest contacts (spaced at about 1000 μm). The line width of the meanderline is 40 μm, and the furrows created by the laser beam are ~15 μm wide. A scanning electron microscope image of a furrow shown in Figure 7 indicates that the morphology of the thin film was dramatically altered by the laser beam. Room temperature resistance measurements of the patterned samples indicate that they have good electrical

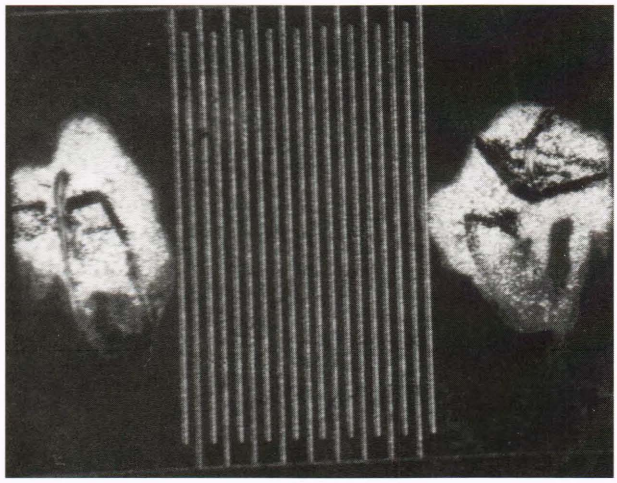

Figure 6. Meanderline pattern etched on a granular yttrium–barium–copper oxide thin film by an argon ion laser. The line width is ~ 40 μm.

isolation and increased resistance over the unpatterned samples (by one to two orders of magnitude). Later, we will show that the microwave response is increased by laser patterning.

Our results indicate that laser patterning will be very useful in optimizing the resistance and response for both the bolometric and nonbolometric detectors. Laser patterning is well suited for working with very small detectors ($2 \times 2 \times 0.125$ mm). Our current system allows us to alternate easily between patterning and detection measurements.

MEASUREMENT RESULTS

Basic measurements of the following four parameters are used to determine thin-film detector characteristics:

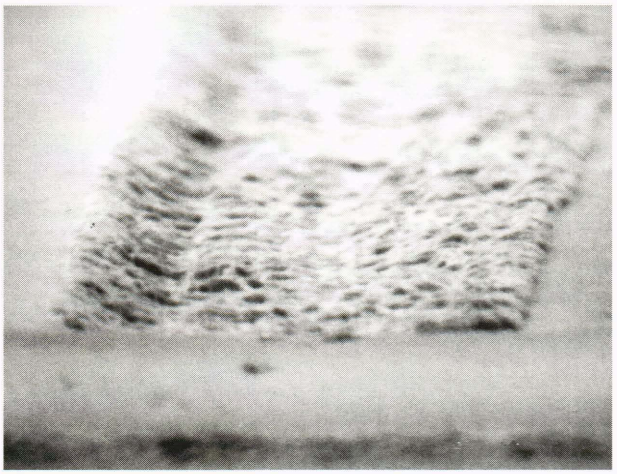

Figure 7. Scanning electron microscope picture of a swath created in a granular yttrium-barium-copper oxide film by the argon laser. The swath width is approximately 15 μm.

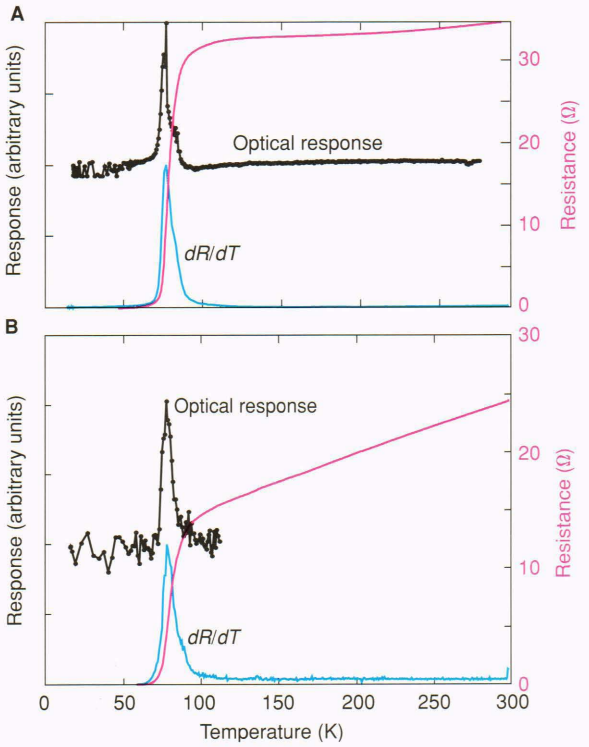

Figure 8. Optical response, resistance, and *dR/dT* (temperature derivative of the resistance curve) versus temperature of two bismuth-strontium-calcium-copper oxide samples. Optical response follows *dR/dT* in both samples, which indicates that they are bolometric. **A.** LAP10F sample (current bias = 1.04 mA, chopping frequency = 40 Hz). **B.** 6005B sample (current bias = 100 μA, chopping frequency = 40 Hz).

dc four-point resistance, optical response, microwave response, and noise voltage. The resistance and microwave response or resistance and optical response are measured simultaneously as a function of temperature, bias current, illumination power, and chopping frequency. The noise voltage is measured as a function of temperature, bias current, and chopping frequency. The responsivity $\Re$, noise equivalent power (NEP), and detector time constant τ can be derived from these measurements. A transient response measurement is also used to measure the time constant of the faster microwave response mechanism.

For optical detection, 4-mW, 633-nm, helium-neon (HeNe) laser radiation is chopped (at 15 Hz to 4 kHz) and focused onto the center of the sample. For microwave response measurements, a 9-GHz microwave signal is generated with a microwave oscillator, square-wave modulated (15 Hz to 50 kHz) with a p-i-n diode modulator, amplified, and fed into an X-band horn positioned directly in front of the sample. In both methods the induced output voltage from the sample is synchronously detected with a lock-in amplifier. The noise measurements are made with the lock-in amplifier at frequencies from 15 Hz to 50 kHz.

Results shown in Figures 8A and 8B for the optical (HeNe laser) detection experiment indicate that the response peaks are located at the center of the resistive transition region (T_c = 82 and 78 K, respectively) and correlate well with derivatives of the resistance curves (*dR/dT*) as expected for bolometric detection. Calculations of responsivity of the LAP10F and 6005B samples yielded relatively low values of 300 mV/W and 10 mV/W with NEP's of 2.0×10^{-5} W/Hz$^{1/2}$ and 9.3×10^{-6} W/Hz$^{1/2}$, respectively. Substrates dominate the overall response times, which were calculated from the lock-in chopper frequency response 3-dB points (47 and 11.5 Hz) to be 5.9 and 24 ms, respectively.

The peak in the microwave response is located in the region of the resistive tail well below T_c, as shown in Figure 9, and is clearly separated from the optical bolometric response peak for the same sample as shown previously in Figure 8. This finding implies that the microwave response is nonbolometric. As expected, the peak of the response and the resistive tail width increased with rising microwave power. At low powers, the response varies linearly with power, and at high powers, the response varies nonlinearly with power. In addition, lock-in response to microwaves does not roll off with chopper frequency (up to 50 kHz) as did the optical response, implying the microwave response mechanism is much faster than the optical response mechanism. Calculated maximum responsivity for the sample response shown in Figure 9 was found to be 136 V/W, which approaches the responsivity seen in conventional diodes. The signal-to-noise ratio was calculated to be 1.85×10^3 at saturation. To extend the measurements of frequency response further, we measured the transient response to a pulsed p-i-n diode microwave source. The estimated fall time of the detected response is about 100 ns as shown in Figure 10.

The microwave response versus temperature for various applied bias current values was also measured and revealed increased responsivity versus bias current and a decrease in the peak location versus temperature as bias current was increased (see Figure 11). These results are qualitatively similar to results reported by Afanasyev et al.[15] on YBCO. Noise voltage measurements were also taken with the lock-in amplifier using a low-noise preamplifier and biasing with a battery source. Similar microwave noise emission results were observed by Konopka

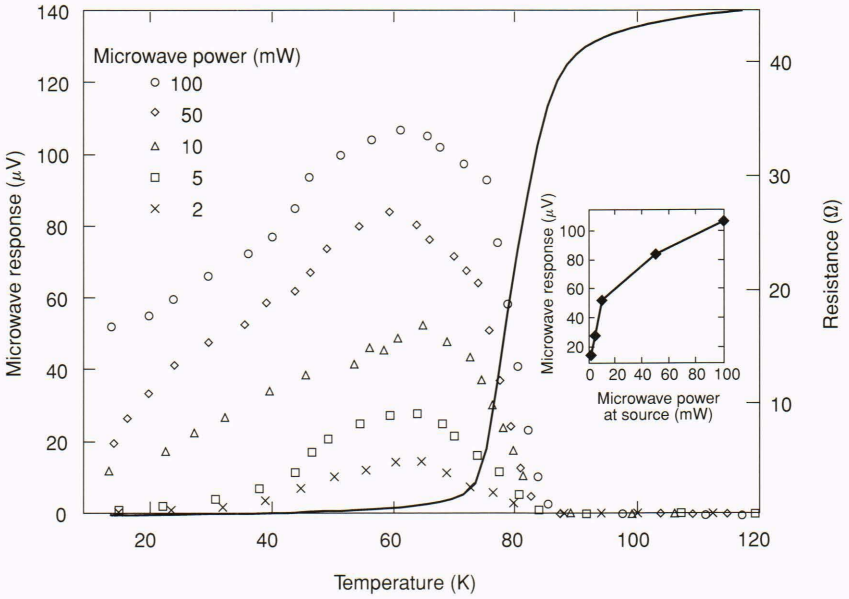

Figure 9. Microwave response (symbols) versus temperature of a bismuth-strontium-calcium-copper oxide sample (LAP10F) for different microwave powers. The inset is a plot of the peak microwave response versus microwave power. The peak response is located in the resistive tail region. The resistance versus temperature curve (solid black curve, 100-mW power) is shown for comparison. (All curves at 249-μA bias. Signal frequency = 9 GHz, chopping frequency = 40 Hz.)

et al. in YBCO films.[7] For our measurements, the equivalent noise bandwidth was set to 1 Hz, and the chopping frequency was set to 40 Hz. Even with no illumination, the sample has a noise peak in the resistive tail region as shown in Figure 12. An NEP of approximately 6×10^{-10} W/Hz$^{1/2}$ was calculated from the measurements using the noise voltage at the peak (at $T \sim 55$ K) for the curve with a 248-mA bias and the estimated responsivity at saturation.

The responsivity and NEP of the bolometric detection mode using HeNe laser light (633 nm) are clearly not very good, although as bolometers the samples (in all fairness) were not optimized. To improve the bolometer response time and NEP, the substrates must be thinned considerably over these samples, as discussed earlier. In contrast, the responsivity of the nonbolometric mode in these same samples using an X-band (9-GHz) source is relatively high (136 V/W) and is independent of modulation frequency up to at least 10 MHz; the NEP is good. Of course, the nonbolometric mode was not optimized either. The means to optimize the nonbolometric response are not yet clear, however, because the exact response mechanism has not been determined.

Our most recent experimental results have shown that the microwave response can be increased by laser patterning. A meanderline was patterned onto a sample using the argon laser. Before patterning, the sample had a room temperature resistance of 5 Ω, metallic behavior above T_c, and a narrow transition width with a small resistive tail. A peak voltage response of 3.378 μV was obtained by illuminating the sample with 50 mW of 8-GHz microwave radiation at a current bias of 5 mA.

After patterning, the resistance properties of the sample changed dramatically. It had a room temperature resistance of 1025 Ω and semimetallic behavior above T_c. Although an abrupt drop in resistance occurred in the transition region, the resistance never went to zero. As the temperature decreased below T_c, the resistance increased exponentially, indicating a semiconductor behavior. The response to microwaves also changed dramatically, giving a peak voltage response of 75 μV for 50 mW of 8-GHz microwave radiation with a current bias of 100 μA. Through patterning, the microwave response increased by a factor of 21.5 with a bias current of only 2% of that before patterning, as shown in Figure 13. It is not clear at this time whether the increase was due to a local alteration of existing grains or an increase in the percolation path caused by the meander pattern.

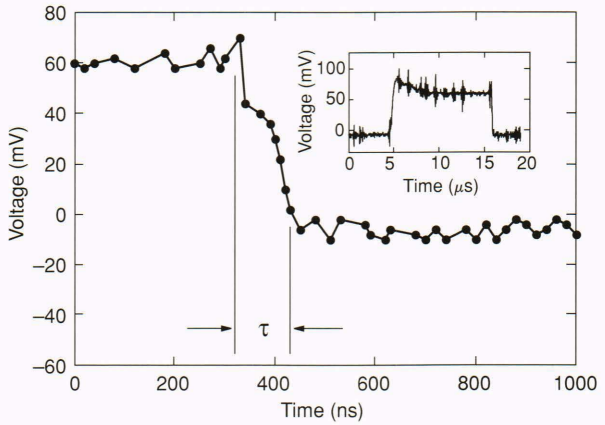

Figure 10. Transient response curve of a bismuth-strontium-calcium-copper oxide sample (LAP10F) to pulsed microwave radiation showing the fall time of the digitized detected pulse. The inset shows the full transient pulse. (Current = 1.0 mA, detector time constant τ = 100 ns, power = 100 mW, signal frequency = 8 GHz, chopping frequency = 40 kHz.)

We have observed that microwave response improves with increasing sheet resistance $R_\square$ and increasing transition width ΔT. Table 1 lists measurement parameters for three films: CVC1, LAP10F, and Z12. The CVC1 film is an epitaxial YBCO film, and LAP10F and Z12 are granular BSCCO and YBCO films, respectively. The CVC1 film has a very small sheet resistance and narrow transition width. Even after using a large microwave power and bias cur-

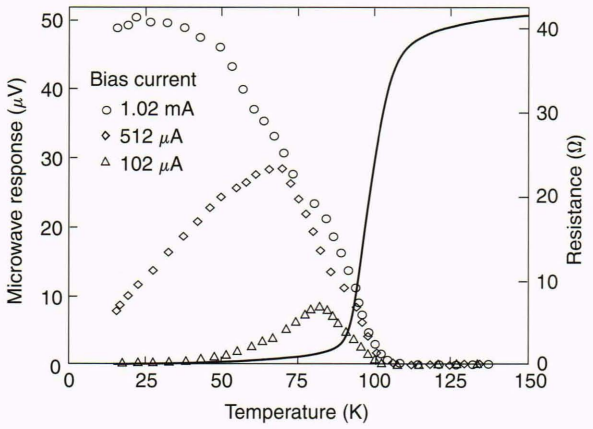

Figure 11. Microwave response versus temperature of a bismuth–strontium–calcium–copper oxide sample (LAP10F) for various applied bias currents at fixed microwave power. The resistance versus temperature curve (solid black curve, 512-μA bias) is shown for comparison. (Power = 5 mW, signal frequency = 9 GHz, chopping frequency = 40 Hz.)

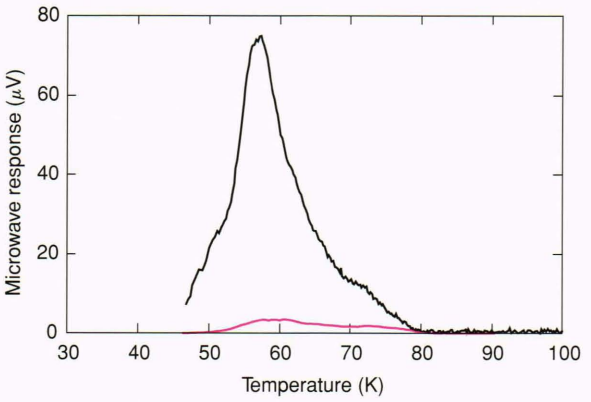

Figure 13. Microwave response versus temperature of a bismuth–strontium–calcium–copper oxide sample (SCC1B) before (red curve) and after (black curve) laser patterning. Bias current before patterning = 5.0 mA. Bias current after patterning = 0.1 mA. The microwave response is greater by a factor of 21.5 after patterning. (Chopping frequency = 50 kHz, microwave frequency = 8 GHz, microwave power = 50 mW.)

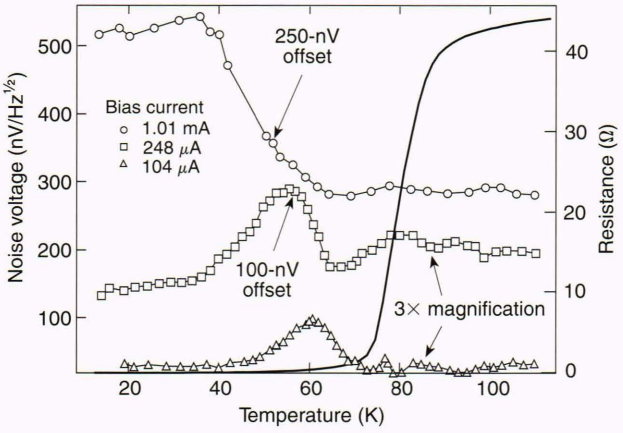

Figure 12. Noise voltage versus temperature for a bismuth–strontium–calcium–copper oxide sample (LAP10F) for various bias currents. The resistance versus temperature curve (solid black curve, 248-μA bias) is shown for comparison.

rent, the microwave response of CVC1 is very small relative to the responses of the granular films. The parameters for the granular films indicate that the microwave response appears to improve with greater sheet resistances and transition widths. Further studies are needed to validate this trend. The implications of these results will be discussed in the next section.

In summary, both nonbolometric and bolometric responses are observed in the same sample. The nonbolometric response occurs for below-gap radiant energy (λ = 3 to 4 cm), and the bolometric response occurs for above-gap radiant energy (λ = 633 nm). The nonbolometric response peak occurs in the resistive tail region, whereas the bolometric response peak follows *dR/dT*. As bias current is increased, the nonbolometric response peak increases in magnitude and moves to a lower temperature. Power dependence of the nonbolometric response crosses over from linear at low incident powers to nonlinear at high incident powers. The nonbolometric response is much faster (τ < 100 ns) than the bolometric response (τ = 5 to 24 ms). The magnitude of the nonbolometric response grows with increasing sheet resistances and transition widths. In the next section, these observations are compared with the work of others in the hope of finding a nonbolometric detection mechanism.

ANALYSIS OF MICROWAVE RESPONSE

Real granular thin-film detectors consist of an ensemble of superconducting grains in which the strength of coupling (and associated critical current) varies widely over the film. When incident radiation couples to such films, the exact mechanism, whether Josephson junction- or vortex-mediated (or a combination of both), is not always clear. To optimize the nonbolometric response of our granular films, however, a model or combination of models that fit our data must be found. Some of the parameters that must be considered are the effect of granularity on response and the sample response versus incident power and wavelength, bias current, temperature, and chopping frequency.

The responses versus temperature and bias current give evidence for the theory of direct coupling of radiant energy to weak links in granular thin films. Our results show a nonbolometric response peak that occurs at a lower temperature and is well separated from the bolometric peak. We also show that the nonbolometric response peak increases in magnitude and moves to a lower temperature with increasing bias current. Results of work by Afanasyev et al.[14,15] and Strom et al.[13,22] are consistent with response versus current measurements taken at APL. Afansyev et al. modeled the granular material as a system of grain-boundary weak links with different critical currents. Their model can account for the position of the nonbolometric peak in the tail region and for the shifting of the peak due to bias current.

The response versus incident power gives additional evidence for the theory of direct coupling of radiant energy to weak links in granular thin films. The character-

Table 1. Comparison of microwave response.

Sample name	Sheet resistance (Ω)	Transition width (K)	Microwave response (μV)	Microwave power (mW)	Current bias (mA)	Normalized response (μV/mA·mW)
CVC1	1.8	2	2	50	3	0.0133
LAP10F	43	9	105	50	0.249	8.43
Z12	127	25	550	2	0.434	633.64

istics of our response to below-gap radiation display a dependence on incident power where there is a transition from linear to nonlinear response at high powers. Strom et al.[13,22] observed a similar response to below-gap radiation, which they attributed to direct coupling of far-infrared light to resistively shunted Josephson junctions. In other words, the detector uses the Josephson effect to produce a detected dc voltage. They have also shown that the nonbolometric response only occurs for below-gap radiant energy, which is also in agreement with our measurements.

Our measurements indicate that the response time of the nonbolometric mechanism is less than 100 ns. The intrinsic response time may be much shorter, since our measurement equipment limits us to 100 ns. Konopka et al.[5] and Yoshisato et al.[16] have estimated response times as short as 40 ps for granular YBCO detectors. They claim such short response times to be a characteristic of Josephson junction detection occurring at grain boundaries.

Investigations at APL of the response characteristics for films with various degrees of granularity and weak-link behavior (and correspondingly different transition widths and sheet resistances) indicate that the granularity of a sample has an effect on nonbolometric detection. Results described earlier showed an increase in response for films with larger sheet resistances and increasing transition widths. Laser-modified films had improved responses, which can be attributed to increases in sheet resistance. Work done by Afanasyev et al.[14,15] also showed that the sheet resistance $R_{\square}$ of a sample has an effect on nonbolometric detection. Films with different numbers of weak-link grains having different coupling (and a correspondingly different $R_{\square}$) were shown to have varied responses, where higher responses were associated with an increase in the sheet resistance.

It is clear that the granularity and associated weak links of a sample have an effect on the response. It is not clear at this point, however, that the increase in response is due solely to Josephson effects. The relative size of the weak links could also allow for the effects of vortices to be felt between grains, whereby more fluxons could pass through the weak link, resulting in resistive losses. Thus, one possible scenario consistent with our results is that the response in these films is due to a combination of Josephson junction- and vortex-mediated responses.

SUMMARY

To date, all of the bolometric measurements have been taken on unoptimized granular HTSC films deposited on substrates with large heat capacities. These films have poor detector characteristics: NEP $\approx 10^{-6}$ W/Hz$^{1/2}$, $\Re \approx$ 0.02 V/W, and $\tau \approx 6$ to 24 ms. If future measurements are performed, they will be on optimized devices consisting of 300-nm epitaxial YBCO films deposited on $2 \times 2 \times 0.125$ mm substrates with small heat capacities. These devices are ready for measurement. An NEP of about 10^{-10} W/Hz$^{1/2}$ and a detector time constant τ of about 10 ms are theoretical detector characteristics for these devices. These devices should compare well with the FTS pyroelectric detector,[34] which has a similar response time and an NEP of about 5×10^{-9} W/Hz$^{1/2}$, but should exceed it in wavelength coverage, extending beyond 100 to 500 μm. In fact, a sensitive infrared HTSC bolometer was recently fabricated by Verghese and Richards.[35] Using an FTS, they showed that their HTSC bolometer is more sensitive than a pyroelectric detector at infrared wavelengths.

The HTSC bolometric detector holds the most promise for use as a far-infrared detector (20 to 1000 μm) in both laboratory and space environments. Currently, only liquid helium (4 K) or room temperature (300 K) detectors are available for the far-infrared band. The achievable sensitivity of an 80- to 90-K HTSC bolometer fills the gap between the more sensitive 4-K and less sensitive 300-K detectors. The use of an HTSC bolometer for a spectroscopic system employed on a mission to the outer planets is currently being evaluated by NASA.[36] Since the mission will take eleven years, only 300-K devices (Golay cell/pyroelectric) will be used, for it is impractical to carry liquid helium for a mission of this length. An HTSC bolometer would be ideal for this mission, since temperatures of 80 to 90 K can be obtained by passive cooling.

Table 2 summarizes the microwave detector characteristics derived from our nonbolometric detection measurements for unoptimized films. These results are compared with characteristics of typical microwave diode detectors and indicate that the nonbolometric detector may be competitive with diode detectors after optimization. Even though our measurements of τ and $\Delta\lambda$ were limited by equipment, measurements performed by others indicate that detection using granular HTSC films is very fast and covers a wide spectral range. Konopka et al.[5] performed a microwave mixing experiment with a granular YBCO film and found that the time constant is less than 40 ps. Strom et al.[13] measured the far-infrared response of a YBCO film and indicated that a nonbolometric response occurs at a wavelength of 385 μm. These investigators believe the high-frequency cutoff for the nonbolometric response is limited by the gap (far infrared). If so, the nonbolometric detector could have inherently subpicosecond speeds and cover a broad spectral band from

Table 2. Comparison of high-temperature superconducting nonbolometric detector to diode detectors.

Detector type	Responsivity (V/W)	NEP ($W/Hz^{1/2}$)	Detector time constant (ns)	Spectral range (GHz)
Diode detectors (typical values)	400 to 1500	10^{-11} to 3×10^{-12}	1 to 10	1 to 18
Unoptimized HTSC microwave detector[a]	100 to 1000	6×10^{-10}	<100	8 to 12

Note: HTSC = high-temperature superconducting.
NEP = noise equivalent power.
[a]Values obtained from measurements.

microwaves to far infrared. We have shown that the responsivity can be increased through patterning. The major issue that remains is whether the intrinsic noise can be reduced through optimization to minimize the NEP.

The HTSC nonbolometric detector may be useful as a wideband power detector or a wideband mixer/demodulator for broadcast or satellite communication equipment.[16] The detector can be passively cooled from 70 to 90 K for space applications. In comparison with a Schottky diode, the nonbolometric detector appears to be very fast, has a large responsivity, and covers a large spectral range. The output impedance of the detector can be controlled easily owing to its planar geometry.

Recently, the nonbolometric microwave response mechanism was modeled and compared with the experimental data described above. Good agreement was found between experiment and theory.[37] The results of this work will be published later.

FUTURE WORK

Many tasks remain to be completed. Although we still hope to test an optimized bolometer and perform FTS measurements, commercial companies such as Conductus, Inc., have now marketed competitive HTSC bolometers for the far infrared. Our remaining interest in the FTS measurements is to obtain thin-film absorption characteristics and nonbolometric response versus wavelength in the range from optical to submillimeter waves. These results should provide information not only about the spectral range of operation but may also provide clues to the origins of the nonbolometric detection mechanism.

We would also like to test and evaluate the broadband spiral antenna/detector, since it could be a practical HTSC device. The antenna/detector should be constructed so that only local cooling of the superconducting element will be necessary rather than the entire antenna. The antenna/detector should also permit a test of the nonbolometric microwave response frequency dependence over the important 2- to 12-GHz range.

Finally, the effects of laser patterning should be investigated. It is hoped that selective laser patterning will help resolve issues regarding the response mechanism in granular HTSC detectors. By locally altering the film morphology in a prescribed fashion, it is hoped that the electrical properties of the film can be closely controlled. In this way, the characteristics of the film can be varied to isolate the fast response mechanism.

REFERENCES

[1]Boone, B. G., *Application of High-Temperature Superconducting Thin-Film Devices to Electro-Optical and Electronic Warfare Systems*, JHU/APL TG 1377 (Feb 1990).

[2]Forrester, M. G., and Talvacchio, J., "Photon Detection by High-Temperature Superconducting Films: Fundamental Limits," *Physica C* **162-164**, 391-392 (1989).

[3]Richards, P. L., Clarke, J., Leoni, R., Lerch, Ph., Verghese, S., et al., "Feasibility of the High T_c Superconducting Bolometer," *Appl. Phys. Lett.* **54**, 283-285 (1989).

[4]Wolf, S. A., " Making Sense of Superconducting Infrared Sensors," *SPIE* **1039**, 253-254 (Dec 1988).

[5]Konopka, J., Sobolewski, R., Konopka, A., and Lewandowski, S., "Microwave Detection and Mixing in Y-Ba-Cu-O Thin Films at Liquid Nitrogen Temperatures," *Appl. Phys. Lett.* **53**, 796-798 (1988).

[6]Konopka, J., Jung, G., Gierlowski, P., Kula, W., Konopka, A., et al., "Interaction of Microwave Radiation with High-T_c Films of Different Microstructures," *Physica C* **162-164**, 1041-1042 (1989).

[7]Jung, G., Konopka, J., Gierlowski, P., and Kula, W., "Microwave Noise Emission from High T_c Thin Films," *Appl. Phys. Lett.* **54**, 2355-2357 (1989).

[8]Moorjani, K., Adrian, F. J., Kim, B. F., Bohandy, J., Phillips, T. E., et al., "High-Temperature Superconductivity," *Johns Hopkins APL Tech. Dig.* **11**(1&2), 155-167 (1990).

[9]Boone, B. G., Sova, R. M., Moorjani, K., Green, W. J., and Grabow, B. E., "Microwave Detection Using Granular Bi-Sr-Ca-Cu-O Thin Films," *J. Appl. Phys.* **69**(4), 2676-2678 (1991).

[10]Rose, K., "Superconducting FIR Detectors," *IEEE Trans. Elec. Dev.* **ED–27**, 118-125 (Jan 1980).

[11]Martin, D. H., and Bloor, D., "The Application of Superconductivity to the Detection of Radiant Energy," *Cryogenics* **1**, 159-165 (Mar 1961).

[12]Richards, P. L., "The Josephson Junction as a Detector of Microwave and Far Infrared Radiation," in *Semiconductors and Semimetals*, Willardson, R. K., and Beer, A. C. (eds.), Academic Press, New York, Vol. 12, pp. 395-439 (1977).

[13]Strom, U., Culbertson, J. C., and Wolf, S. A., "Far Infrared Photoresponse of Two-Dimensional Granular YBaCuO Films," *SPIE* **1187**, 290-294 (1989).

[14]Afanasyev, A. S., Divin, Y. Y., Gubankov, V. N., Shadrin, P. M., and Volkov, A. F., "Response of YBaCuO Thin Films to Millimeter-Wave Electromagnetic Radiation," in *Proc. Int. Conf. on Millimeter Waves and Far-IR. Tech.*, McMillan, A. S., and Tucker, G. M. (eds.), Beijing, China, pp. 44-47 (Jun 1989).

[15]Afanasyev, A. S., Volkov, A. F., Gubankov, V. N., Divin, Y. Y., and Shadrin, P. M., "Response of YBaCuO Thin Films to Electromagnetic Radiation and Their Electrical Characteristics," *IEEE Trans. Mag.* **25**(2), 2571-2574 (Mar 1989).

[16]Yoshisato, Y., Takeoka, A., Ikemachi, T., Niki, K., Yokoo, T., et al., "Microwave Detector Using Granular-Type YBCO Superconductors," *Jpn. J. Appl. Phys.* **29**(6), 1080-1085 (Jun 1990).

[17]Zeldov, E., Amer, N. M., Koren, G., and Gupta, A., "Nonbolometric Optical Response of $YBa_2Cu_3O_{7-d}$ Epitaxial Films," *Phys. Rev. B* **39**, 9712-9714 (1989).

[18]Gallop, J. C., Radcliffe, W. J., Langham, C. D., Sobolewski, R., Kula, W., et al., "Josephson Effects and Microwave Response of HTS Thin Films," *Physica C* **162-164**, 1545-1546 (1989).

[19]Strom, U., Culbertson, J. C., and Wolf, S. A., "Light Detection Using Superconducting Films," in *Proc. Workshop on High-Temperature Superconductivity*, GACIAC PR-89-02, Huntsville, Ala., pp. 219-227 (May 1989).

[20]Kadin, A. M., Leung, M., Smith, A. D., and Murduck, J. M., "Infrared Photodetector Based on the Photofluxonic Effect in Superconducting Films," *SPIE* **1477**, 156-165 (4 Apr 1991).

[21]Culbertson, J., Strom, U., Wolf, S. A., Skeath, P., West, E. J., et al., "Nonlinear Optical Response of Granular YBaCuO Films," *Phys. Rev. B* **39** (16), 12,359-12,362 (1 Jun 1989).

[22]Strom, U., Culbertson, J. C., and Wolf, S. A., *SPIE* **1240**, 516-517 (26 Oct 1989).

[23]Clarke, J., Hoffer, G. I., Richards, P. L., and Yeh, N. H., "Superconductive Bolometers for Submillimeter Wavelengths," *J. Appl. Phys.* **48**(12), 4865-4879 (Dec 1977).

[24]Richards, P. L., Verghese, S., Geballe, T. H., and Spielman, S. R., "The High T_c Superconducting Bolometer," *IEEE Trans. Mag.* **25**(2), 1335-1338 (1989).

[25]Hadni, A., *Essentials of Modern Physics Applied to the Study of the Infrared*, Pergamon Press, Paris, pp. 252-257 (1967).

[26]Meitzler, R. C., *Bolometric Detection Using High Temperature Superconductors*, JHU/APL F1F(1)-89-U-253 (1989).

[27]Nahum, M., Hu, Q., and Richards, P. L., "Fabrication and Measurement of High T_c Superconducting Microbolometers," *IEEE Trans. Mag.* **27**(2), 3081-3084 (Mar 1991).

[28]Kim, B. F., Bohandy, J., Moorjani, K., and Adrian, F., *AIP Conf. Proc.* **165**, 182 (1987).
[29]Sova, R. M., *A Survey of Techniques to Deposit Thin Films of High Temperature Superconducting Ceramics*, JHU/APL F1F(1)-89-U-004 (1989).
[30]Stucki, F., Bruesch, P., and Baumann, Th., "XPS Study of the Grain Boundary Phase in $YBa_2Cu_3O_{7-x}$," *Physica C* **156**, 461-466 (1988).
[31]Grabow, B. E., Sova, R. M., Boone, B. G., Moorjani, K., Kim, B. F., et al., in *Proc. AMSAHTS '90—Advances in Material Science and Applications of High Temperature Superconductors*, NASA Goddard Space Flight Center, Greenbelt, Md., pp. 307-316 (2-6 Apr 1990).
[32]Rothschild, M., Sedlacek, J. H. C., Black, J. G., and Ehrlich, D. J., "Laser Patterning of Metal Oxide Superconductor Films by Reactive Solid-State Transformation," *IEEE Trans. Electron Device Lett.* **9**, 68 (1988).
[33]Liberts, G., Eyett, M., and Bauerle, D., "Direct Laser Writing of Superconducting Patterns into Semiconducting Ceramic Y-Ba-Cu-O," *Appl. Phys. Lett. A* **46**, 331 (1988).
[34]Pyroelectric Detector for DA3 FTS, BOMEM, Inc., Spectrometer System Description Catalog, Quebec, Canada (1988).
[35]Verghese, S., and Richards, P. L., "Fabrication of an Infrared Bolometer with a High T_c Superconducting Thermometer," *IEEE Trans., Mag.* **27**(2), 3077-3080 (1991).
[36]Brasunas, J., Kunde, V., and Moseley, H., "Upcoming Planetary Missions and the Applicability of High Temperature Superconductor Bolometers," in *Proc. AMSAHTS '90—Advances in Material Science and Applications of High-Temperature Superconductors,* NASA Goddard Flight Center, Greenbelt, Md., pp. 449-458 (2-6 Apr 1990).
[37]Grabow, B. E., *Microwave and Optical Detection Using Granular Bi-Sr-Ca-Cu-O Thin Films*, Ph.D. dissertation, The Johns Hopkins University (1992).

ACKNOWLEDGMENTS: This work has been supported by APL independent research and development. We would like to thank the following APL staff members for their important contributions to the project: Kishin Moorjani and Bill Green for supplying us with superconducting films; Rick Edwards and Liz Dettmer (former employee) for help in developing patterning and contact deposition techniques; and Don Duncan, Terry Harris, and Tom Cotter for their contributions in the development of the laser patterning system. We would also like to thank Tom Hughes (former graduate student) and Ali Razavi of Wilkes University for supplying us with films and to acknowledge Tom's efforts in the development of the laser patterning system. Finally, we would like to thank Rich Meitzler of The Johns Hopkins University for his work in modeling the bolometric detector.

THE AUTHORS

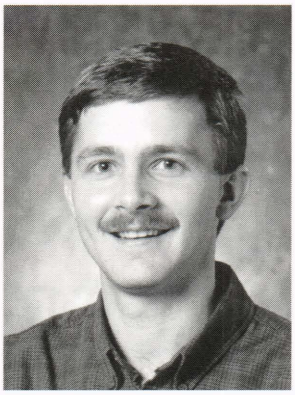

RAYMOND M. SOVA received his B.S. in electrical engineering from the Pennsylvania State University and his M.S. in applied physics from The Johns Hopkins University. He is currently pursuing a Ph.D. in electrical engineering from The Johns Hopkins University. He is a member of APL's Electro-optical Systems Group, where he has worked on the development of a digital signal processing algorithm for electronically scaling and rotating digital images and the development of high-temperature (>77 K) superconducting thin-film radiation detectors. Current research interests include the development of a laser remote sensing system for measuring atmospheric humidity and temperature profiles and spectroscopic studies of oxide materials and atmospheric gases.

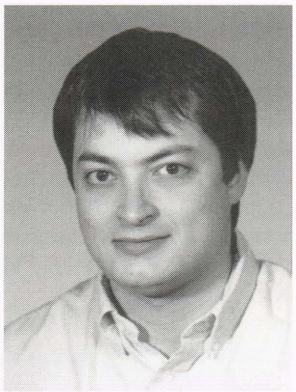

BARRY E. GRABOW received his B.S. in electrical engineering from the Milwaukee School of Engineering in 1987 and an M.S. and Ph.D. in electrical engineering from The Johns Hopkins University in 1990 and 1992, respectively. He is presently teaching at The Johns Hopkins University for the Part-time Programs in Engineering and Applied Sciences and holds a postdoctoral position in the Electrical and Computer Engineering Department of The Johns Hopkins University. Dr. Grabow's current interests include superconductivity, microwaves, optics, and solid-state physics. He holds memberships in Tau Beta Pi, Eta Kappa Nu, and Delta Sigma Phi and is a student member of the IEEE.

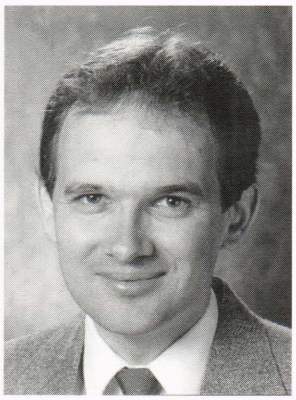

BRADLEY G. BOONE is supervisor of the Image and Signal Processing Section of APL's Electro-optical Systems Group. He received his Ph.D. degree from the University of Virginia in 1977, working in superconducting electronics with Bascom S. Deaver. Since joining APL in 1977, he has worked on a variety of projects related to lasers, optical and infrared sensors, imaging radar, optical pattern recognition, and high-temperature superconductivity. Dr. Boone is currently developing a novel optical/digital processor for pattern recognition and working with the Wilmer Eye Institute on measuring retinal thickness for early detection of blinding retinal diseases. He is a member of the faculty of The Johns Hopkins University G.W.C. Whiting School of Engineering and was a William S. Parsons visiting professor in the Electrical and Computer Engineering Department of JHU in 1991.